Transportation Geotechnics 48 (2024) 101326

Contents lists available at ScienceDirect

Transportation Geotechnics

journal homepage: www.elsevier.com/locate/trgeo

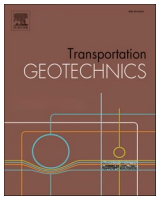

Original Article

Chemical, mineralogical and geotechnical properties of volcanic ash of Tajogaite (La Palma, Canary Islands, Spain)

Svetlana Melentijević [a,*], Sol López-Andrés [b], José Estaire [c]

[a] Department of Geodynamics, Stratigraphy and Palaeontology, Faculty of Geological Science, Universidad Complutense de Madrid, Madrid, Spain
[b] Department of Mineralogy and Petrology, Faculty of Geological Science, Universidad Complutense de Madrid, Madrid, Spain
[c] Laboratorio de Geotecnia (CEDEX), Madrid, Spain

ARTICLE INFO

Keywords:
Volcanic ash
Chemical and mineralogical analysis
Geotechnical characterization
One-dimensional consolidation test
Direct shear test

ABSTRACT

Volcanic eruption at La Palma island (Tajogaite, 2021) has produced tons of volcanic ash as natural sediments spread all around the island covering existing crops, roads, embankments, buildings, etc., by that way producing damage to environment. For the rehabilitation and reconstruction of island, and its application to adjacent areas, it is practical and economical to employ these volcanic ashes as construction material being encountered in abundant volume, and by that way could be considered as a resource material instead as a waste material, reducing necessary volume of landfills for its deposition. This paper defines the investigation of chemical, mineralogical and geotechnical properties of these deposited materials for its possible reuse by that way providing solution for its recovery. These young volcanic ashes are studied in its fresh natural state, prior to consolidation and cementation has taken place for its chemical, mineralogical and geotechnical characterization. Volcanic ash of Tajogaite is of a poorly graded sandy nature having difficulties for its compaction, having low improvement of relative density by the application of standard compaction methods. Mineralogy analysis indicates it is rich in silica, iron, calcium and alumina oxide, although being necessary the addition of mineral additives for its alkali-activation. Geotechnical characteristics of different samples vary depending on the sampling site, being resistance parameters determined by direct shear test (friction angle 30° to 34°) and deformational properties defined by one-dimensional consolidation test considered low values as of loose sand materials (deformation modulus range from 20 to 40 MPa).

Introduction

In recent years, the volcanic activity has increased all around the world, in particular in the last couple of years the following important volcano eruptions has been noticed: Stromboli and Etna, Sicily, Italy; Mauna Loa, Hawai, USA; Semeru, Indonesia; Villarica, Chile; Popocatépetl, México; Fagradalsfjall, Iceland; Sakurajima, Japan; Bulusán, Philippines; and Hunga Tonga, Pacific Ocean [62].

After intensive seismic activity and large ground deformations, the volcanic eruption of Tajogaite (Cumbre Vieja on La Palma island, Canary Islands, Spain) in 2021, being active for more than 3 months [41,47]. During last volcanic eruption, deposition of volcanic materials has affected many different constructions, having negative impact both on urban and rural areas, destroying lots of buildings, family houses, roads, geotechnical structures, crops, etc. Different types of volcanic waste materials (volcanic blocks, lapillus, coarse and fine volcanic ash) in large quantities have been deposited all over La Palma island that had to be considered for its placement in different landfills being by that way a huge environmental problem for the island. The main waste material, as the product of volcanic activity, is the volcanic ash which was estimated at around 200 million m^3 [8]. It is considered a hazardous residue resulting from the volcanic activity produced in large quantities being a subject of problematic decision for the waste disposal at limited landfills situated at this small island. According to several researchers, in general there is no European legislation regarding disposal and recycling of volcanic ashes being classified in general as “Municipal residue” and “street-cleaning residues”[10].

It is of great importance to make use of the volcanic ash, being an environmental problem its storage, classified as a waste material to be stored, instead to be used as a resource for geotechnical engineering being available at site in abundant quantity and due to economic considerations.

Volcanic ash are pyroclastic vitreous materials produced during volcanic eruptions. They can be found in enormous quantities in areas

* Corresponding author.

https://doi.org/10.1016/j.trgeo.2024.101326
Received 29 December 2023; Received in revised form 26 July 2024; Accepted 27 July 2024
Available online 30 July 2024

with current and past volcanic activities and they are considered as a natural waste material of low economic cost. Their use as an alternative material in the construction industry and in geotechnical applications is gaining importance in recent years, being an alternative source to the use of fly ash from thermal plants, as well as for reducing the use of cement as principal construction material for increasing demand in the growth of urban areas due to necessity for reduction of emission of carbon dioxide.

There are a lot of volcanic soils all around the world, whose finest part defined as volcanic ash is classified as sandy soils, whose chemical and mineralogical characterization is extensively analyzed [53,1,26,42,47,33]. Geotechnical properties of young volcanic deposits where no consolidation and cementation has yet taken place are in general less studied than of conventional sandy soil type [39,4,7], although there are more studies on old volcanic ash deposits [53,23,38,36,49,40,43,46]. Considering that there is little information on geotechnical properties of young volcanic deposits, in this paper the study of freshly deposited volcanic ash is presented. This paper focuses on mineralogical, chemical and morphological characterization of volcanic ash of Tajogaite, and further geotechnical analysis for its general characterization. Geotechnical laboratory tests are carried out to characterize and define its gradation curves, index properties, deformation and strength parameters, possible collapsibility and particle crushing.

Volcanic ash can be used for geotechnical structures by its application as binder for soil stabilization of deficient materials (infrastructures such as base and subbase of roads, foundation and construction of embankments, foundation of buildings, etc.). Studies on the utilization of volcanic ashes for the stabilization and improvement of geotechnical properties of deficient soils are limited, the principal publications are founded in the last 10 years for the application of volcanic ash in Italy, Iran, Papua New Guinea, etc. [22,44,56,21,20,37,51]. The general review on natural volcanic pozzolans as worldwide resource material presented in Robayo-Salazar and Mejía de Gutierrez [45] indicates that there is still low number of scientific researches regarding its application as alkali-activated geopolymers, although results obtained demonstrate its possible use as sustainable raw material. The study of Tajogaite volcanic ash as pozzolan material for the use as alkali-activated geopolymer is presented in Presa et al. [42] and Mañosa et al. [33].

There are other studies performed in recent years, a lot of studies were performed on the use of volcanic ash in the construction industry, being introduced in the studies for the cement and mortars production [5,9,19,26,27,29,30,42,47,52,55,64,65] etc, asphalt production [32], as well as fabrication of ceramics and bricks [6,10,30,50,63], etc.

Materials

The volcanic ash (VA), object of this study, is a product of the volcanic eruption that occurred on La Palma island in 2021. Fig. 1 shows the position of La Palma Island in Atlantic Ocean, as well as the position of all collected samples (C0, CS, C1, C2, C3, C4, CJ) in comparison to the location of emission of the volcanic activity. Fig. 2 shows photos of the appearance of different urban and non-urban areas where some of the studied samples of VA (denominated as C1, C2, C3 and C4) were collected at different distances from the volcano eruption during and after the eruptive period. It can be observed the black powdery aspect of VA attributed to high content of iron oxides, with particles less than 2 mm in size. The detailed chemical, mineralogical and morphological analysis of sample CS for its use as raw material to obtain zeolites is performed in Martinez [35].

All material collected for the analysis in this study is taken from the surface, till depth of 20 cm and later reconstituted for laboratory testing. Samples C0, CS, C1, C2 C3 and C4 were collected after the second phase of the volcanic eruption (approximately 2 to 3 months after the beginning of the volcano eruption that occurred on 19th of September of 2021), except sample CJ which was collected 18 months after the end of the eruption. These materials, collected mainly in the short period at

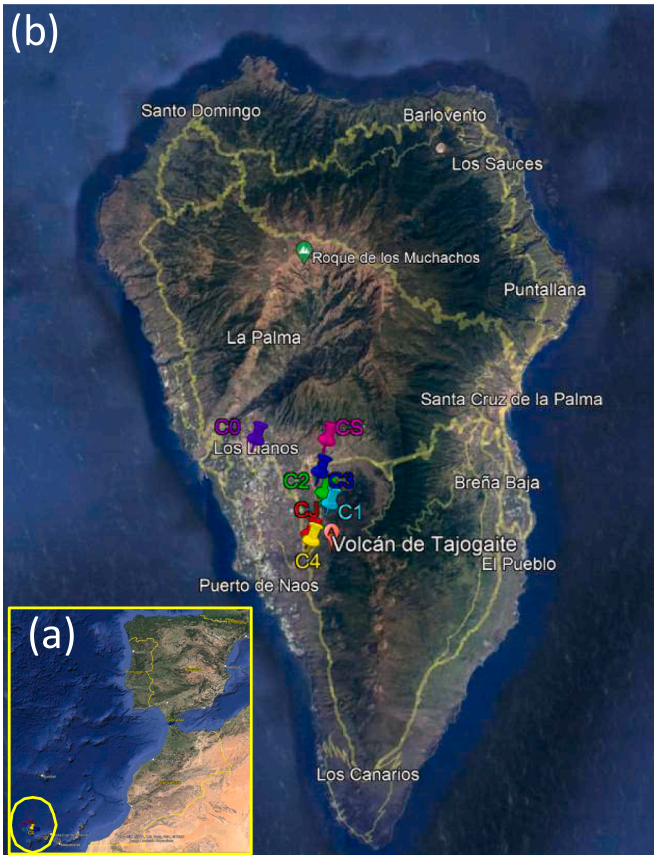

Fig. 1. (a) Position of La Palma island in the Macaronesia and (b) location of collected VA samples with respect to Tajogaite volcano.

volcano eruption, are analysed in its natural state, as freshly deposited material with no consolidation nor cementation that could have been produced.

The samples were subsequently homogenized and quartered in the laboratory to perform necessary tests for chemical, mineralogical and morphological characterization summarized in Table 1 at Geological Techniques Research Assistance Unit belonging to the Center for Research Assistance in Earth Sciences and Archaeometry (UCM), and for geotechnical characterization in Table 2 at Geotechnical Laboratory of the Faculty of Geology (UCM) and at Laboratorio de Geotecnia-CEDEX (Madrid, Spain). Table 1 also includes the distance to the center of the volcano eruption, while Table 2 also summarizes the standards applied for the performance of geotechnical tests.

Chemical, mineralogical and morphological characterization

Mineralogical characterization was carried out by X-ray diffraction (XRD) by the polycrystalline powder method using a BRUKER D8-Advance diffractometer with Cu Kα radiation and graphite monochromator, in an angular range of 2 to 60° of 2θ, a step size of 0.02° and a time per step of 1 s. The identification and semi-quantification of the crystalline phases was carried out with the EVA DIFFRAC plus 13.0 program with the PDF2 (Powder Diffraction File) database of the ICDD (International Center for Diffraction Data). The percentage of amorphous phase was calculated using the software XPowder software version 12[34]. Table 3 shows the semi-quantification by XRD of different VA samples, presenting as well the average values of all samples and also the average values excluding CS and CJ considering its high amorphous phase and collection date in comparison to other samples.

The chemical composition has been determined by X-ray fluorescence (XRF) in a BRUKER S2 Ranger for major and minor elements in

Fig. 2. Images of VA produced by eruption of Tajogaite volcano (Places where samples (a) C1, (b) C2, (c) C3, (d) C4 were collected, respectively) (courtesy Professor Eumenio Ancochea).

Table 1
Laboratory tests performed for chemical, mineralogical and morphological characterization of VA.

Sample	C0	CS	C1	C2	C3	C4	CJ
Distance from the center of volcanic activity (m)	6.950	4.175	1.200	1.900	3.150	1.850	4.847
X-Ray Diffraction (XRD)	X	X	X	X	X	X	X
X-Ray Fluorescence (XRF)	X	X	X	X	X	X	X
SEM-EDX		X	X	X	X	X	X
pH		X	X	X	X	X	X
Conductivity		X	X	X	X	X	X
Loss on Ignition (LOI)	X	X	X	X	X	X	X

Table 2
Laboratory tests performed for geotechnical characterization of VA.

Test	Standard	Samples						
		C0	CS	C1	C2	C3	C4	CJ
Grain size distribution (sieve and laser)	EN ISO 17892–4	X	X	X	X	X	X	X
	ISO 13,320	X	X	X	X	X	X	X
Specific gravity of solid particles (water and gas pycnometer)	EN ISO 17892–3		X	X	X	X	X	X
			X					
Natural water content	EN ISO 17892–1		X	X	X	X	X	
Minimum and maximum density	UNE 103–105 UNE 103–106		X					
Compaction test	UNE 103–500		X	X	X	X	X	
One-dimensional consolidation test	EN ISO 17892–5		X	X	X	X	X	X
Collapse test	UNE 103–406		X	X	X	X	X	X
Direct shear test	EN ISO 17892–10			X	X	X	X	

pellet. The "Loss On Ignition" (LOI), has been previously determined in all cases for the fitting of the chemical analysis. The chemical analysis of the samples, expressed as % by weight (Wt %) of oxides, is shown in Table 4. It also presents the average weight of all samples, as well as average of samples C0, C1 to C4, excluding CS and CJ.

It can be observed in Table 4 that the most critical components of VA are silica (SiO_2), being the main component at approximately 40 %, ferric oxide (Fe_2O_3) consisting of 11 to 15 %, calcium oxide (CaO) ranging from 10 to 14 %, alumina (Al_2O_3) ranging from 10 to 14 % and magnesium oxide (MgO) in order of 6 to 8 %. Other major components are titanium oxide (TiO_2), sodium oxide (Na_2O) and potassium oxide (K_2O). The content of Fe_2O_3 of the sample CJ collected 1.5 years after the volcanic eruption is lower than for other samples collected recently after the eruption, while the content of MgO is greater and TiO2 is lower compared to other samples being exposed to atmospheric agents for longer period. Other components of the sample CJ do not present significant changes in comparison to the recently collected samples during volcanic activity. The average chemical composition is also presented for samples collected in the short period after the volcano eruption, i.e. C0, CS and C1 to C4. The indicated composition shows the presence of typical VA minerals of Tajogaite eruption, such as indicated in Table 3 [8].

According to ASTM C618 (2019), the critical requirements to determine the class of the pozzolanic activity are the content of acid oxides $SiO_2 + Al_2O_3 + Fe_2O_3$, the content of $SO_3 < 4$ %, moisture content < 3 % and LOI<10 %. For the studied samples, the sum of acid oxides makes up to the range from 65 to 70 % (see Table 4), being close to the limit value for its classification as class N or class F materials with pozzolanic properties, being these values in accordance with recently published studies [47,33]. Considering low sulfur content (SO_3), it is considered that should not have an expansion potential when applied to different material combinations as binder material [2]. Due to low value of LOI, considered almost zero, is attributed to the oxidation of the material's iron-bearing phases following thermal treatment [61].

The analysis regarding the composition of magma has the influence on the mineral content of VA, being in this case considered of high crystalline phase, being the amorphous phase low (ranging from 6 to 22 %), except for sample CS having 40.1 % amorphous phase (see Table 3). According to review presented by Jativa et al. [26], having low amorphous phase, being the criteria set at a minimum of 36 %, except for sample denominated as CS, is considered as not suitable for alkali-activated geopolymer production. This deficiency could be overcome by adding different mineral additive such as lime, granulated blast furnace slag, metakaolin, fly ash, etc., in order to compensate for the SiO_2, Al_2O_3 and CaO. On the other hand, based on relation SiO_2/Al_2O_3, it is considered that reactive materials with $SiO_2/Al_2O_3 < 3.9$ are suitable for geopolymer production [45,26] being this condition fulfilled for VA in this study.

Morphological observations and microanalysis (SEM-EDX) have been performed on a TESCAN Vega 4 (high/low vacuum) Scanning Electron Microscope equipped with two Bruker EDX detectors with an accelerating voltage of 20 kv. Sample was deposited on graphite tape and metallized with gold. Fig. 3 presents SEM microscopic images of different studied VA samples under general at 100X and detailed view at more magnification for further discussion of its morphology, grain size, porosity, etc. Microscopic images with secondary (SE) and backscattered electron (BSE) detectors are performed for samples CS, C1 to C4 and CJ. The images on the left (Fig. 3a, c, e, g, i, k) are general views at 100X magnification with ES and the images on the right (Fig. 3b, d, f, h, j, l) are detail views obtained with BSE (CS, C3 and CJ) and with SE (C1, C2 and C4) and at magnifications of 250X, 450X, 240X, 650X, 240X and 350X, respectively. Particle size analysis is determined by gradation curve (see section 4.2) and observed by SEM. The ashes with the largest

Table 3
Amorphous and crystalline phases characterization by XRD (Tr < 0,5%).

Sample		C0	CS	C1	C2	C3	C4	CJ	Average All samples	Average Samples C0, C1 to C4
% Amorphous phase		22	40	9	16	13	11	7	17.0	13.2
% Crystalline phases		78	60	91	84	87	89	93	83.0	86.8
Crystalline phases (%)	Olivine 72–2461	7	8	23	18	19	13	22	15.7	16.8
	Diopside 72–1497	29	23	40	10	37	31	26	27.9	28.8
	Kaersutite 44–1450	2	8	2	4	3	3	5	4.1	3.4
	Ti-Magnetite 75–1376	7	5	8	10	5	8	3	6.7	6.9
	Ilmenite 75–1203	1	3	1	2	1	2	1	1.6	1.3
	Hematites 72–0469	2	3	1	2	1	2	Tr	1.6	1.3
	Labradorite 33–1417	52	50	25	54	34	41	43	42.5	41.4

Table 4
Chemical composition determined by XRF.

Sample	C0	CS	C1	C2	C3	C4	CJ	Average All samples	Average Samples C0, C1 to C4
Oxides	Wt %								
SiO_2	40.23	40.87	40.63	40.80	40.62	40.79	41.79	40.82	40.61
Fe_2O_3	14.23	15.13	15.34	15.41	15.55	15.34	11.44	14.63	15.17
CaO	11.11	10.73	13.73	13.69	13.43	13.67	12.44	12.69	13.13
Al_2O_3	11.35	10.37	13.24	13.47	13.71	13.53	13.43	12.73	13.06
MgO	7.30	7.10	6.80	6.20	5.80	6.40	8.30	6.84	6.50
TiO_2	6.80	5.70	3.92	4.02	4.09	4.03	3.59	4.59	4.57
Na_2O	3.42	3.48	3.20	3.10	3.20	3.10	4.10	3.37	3.20
K_2O	2.48	2.87	1.73	1.77	1.89	1.76	2.38	2.13	1.93
P_2O_5	0.71	0.99	0.55	0.60	0.64	0.59	0.91	0.71	0.62
SO_3	0.72	0.36	0.19	0.24	0.33	0.23	0.56	0.38	0.34
Cl	0.31	0.38	0.15	0.17	0.19	0.17	0.44	0.26	0.20
SrO	0.01	0.07	0.13	0.14	0.15	0.14	0.11	0.11	0.11
Cr_2O_3	0.17	0.20	0.10	0.10	0.09	0.09	0.10	0.12	0.11
MnO	0.08	0.08	0.08	0.08	0.08	0.08	0.09	0.08	0.08
SnO_2	–	0.01	–	–	–	–	0.09		
ZrO_2	0.06	0.08	0.05	0.05	0.05	0.05	0.08	0.06	0.05
V_2O_5	–	–	0.04	0.05	0.07	0.05	0.12	0.07	0.05
ZnO	0.02	0.02	0.01	0.01	0.01	0.01	0.02	0.01	0.01
NiO	0.01	–	0.01	0.01	0.01	0.01	0.02	0.01	0.01
CoO	–	–	0.01	–	–	–	0.05	0.03	0.01
CuO	0.02	0.01	0.01	0.01	0.01	0.01	–	0.01	0.01
PbO	–	–	–	0.03	–	–	–	–	–
MoO	–	–	–	–	–	–	0.01	–	–
CdO	–	–	–	–	–	–	0.05	–	–
Sb_2O_3	–	–	–	–	–	–	0.06	–	–
LOI	–	–	−0.46	−0.37	−0.51	−0.45	−0.51	–	–

particle size and heterogeneous distribution are CJ and C4, while C3 has the smallest and most homogeneous particle size. The most similar samples are C1, C2 and CS. The particles observed by SEM are mainly those of glassy materials. All the particles present a vacuolar morphology with shapes ranging from angular in CS, C1 and C4 to very angular in C2 and C3, typical of volcanic ashes. The density of the vacuoles varies from lower in C3, C1 and C4 to higher in C2 and CS. In addition, the CS sample shows particles with fluid morphology. The CJ sample, sampled 1.5 years after the end of the eruption, shows the least angular morphology with very rounded edges and a texture with high vacuole density which can lead to porosity.

The pH and Electrical Conductivity (EC) of VA samples were measured with a pH-Meter Crison Basic 20 and a Crison Micro CM 2200 conductimeter. Samples were measured according to the protocol of the International Volcanic Health Hazard Network, [24 54]. Table 5 summarizes average values of pH and conductivity performed according to the standard [11,13]. Values of pH ranges from 6.60 to 7.02 indicating the necessity of the addition of additive in order to reach 12.4 as required for the soil stabilization for the pozzolanic activation for the use as geopolymer [13]. Values of electrical conductivity ranges from 22 to 68 μs/cm for different samples, being the lowest for C2 and the greatest for C3 sample, being these values indicative for low proportion of the soluble salts in VA that were not detected by XRD but detected by XRF (low content of Cl and SO_3) and SEM-EDX (presence of F and Cl).

Geotechnical characterization

Test procedures

The geotechnical characterization consisted of the analysis of the grain size distribution (sieve analysis by EN ISO [16] and laser analysis [25]) and compaction tests [60], prior to performance of static geotechnical characterization by determination of deformational characteristics by incremental loading one-dimensional consolidation tests [18] and resistance properties by direct shear test [17]. The possible collapsibility of samples is evaluated by [59] in the consolidometer due to possible collapsible nature of the soil being the material of low dry unit weight with low natural water content. Particle crushing evaluation is performed after performance of one-dimensional consolidation tests. The minimum and maximum unit dry weight of VA is also determined, in order to evaluate the densest and the loosest state of the VA material to be reached, in this case it is only performed for the sample CS according to standards applicable to sandy soils. Namely, UNE 103–105 (pouring VA through a funnel to a specific mold) and [57] (applying the ramming method) are applied, respectively. The summary of performed tests is given in Table 2. The results of mentioned tests are considered

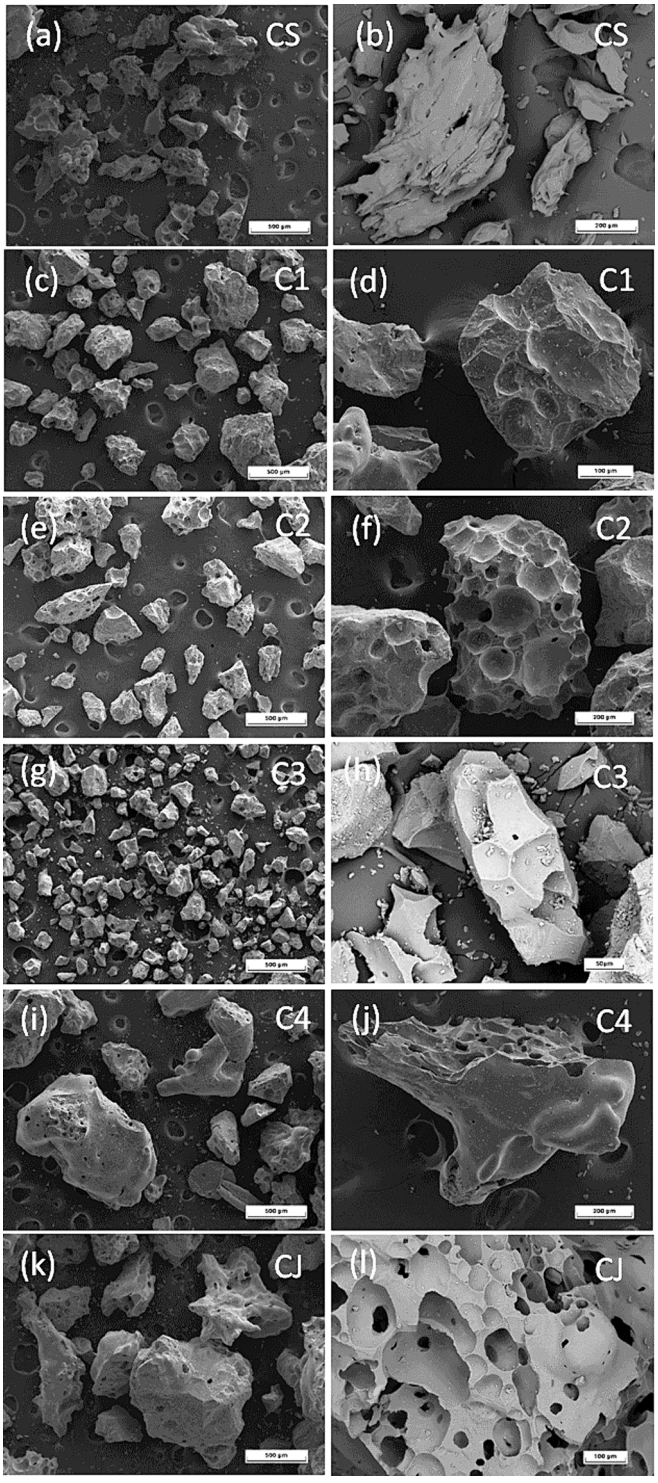

Fig. 3. SEM microscopic images of collected VA samples (a), (b) CS, (c), (d) C1, (e), (f) C2, (g), (h) C3, (i), (j) C4 and (k), (l) CJ.

Table 5
Results of pH and conductivity analysis.

Sample	CS	C1	C2	C3	C4	CJ
pH	6.69	6.90	7.02	6.84	6.60	6.80
Conductivity (μs/cm) 25 °C	32	38	22	68	52	35

interesting for the possible reuse of these materials for different geotechnical purposes.

Grain size distribution and index properties

Grain size distribution analysis is performed according to sieve analysis for the grain size greater than 700 μm combined with laser technique by apparatus Honeywell Microtrac X100 for the grain size lower than 700 μm. Fig. 4 summarizes all gradation curves obtained for all samples under virgin conditions defined as undisturbed samples prior to compaction, and performance of direct shear and one-dimensional consolidation tests, as well as under disturbed conditions after testing for samples CS, C1 to C4, that will be further discussed in Section 4.7.

The analysis for the soil classification of the material performed for samples CS, C0, C1 to C4 and CJ is summarized in Table 6 where the grading and soil classification is defined according to Unified Soil Classification System (USCS) (Fig. 4). It can be observed that all gradation curves show poorly graded sandy material (SP) with fines content (passing through sieve 0.063 mm) ranging from 0.4 to 18.3 %, being samples C0 and CS the ones with the highest content of fines (15.6 to 18.3 %), while other samples have the range of fines content from 0.4 to 5.5 %. Grading parameters determined by gradation curves, consider that the value of the uniformity coefficient (C_u) varies from 2.3 to 4.9 indicating wide range of particle size, while the value of coefficient of gradation (C_z) ranges from 1.0 to 2.1. Samples C1, C2, C4 and CJ are considered lightly gap-graded (missing fraction between 0.2 and 0.4 mm). It can be concluded that in general all curves present more than 97 % of sandy material (<2 mm), being only these particles selected for further analysis of geotechnical properties (resistance and deformation characterization).

It can be observed that in general in the range of sandy materials the gradation curves present variability regarding grain size and different fines content, being collected at different locations and different time period. Also within the same location of the collected samples, a variability in gradation curve can be observed regarding general grain size as well as the fines content. Other studies of freshly deposited VA classifies it of a sandy nature, such as in Orense et al. [39] where a range of gradation curves is observed depending on the distance from the emission of volcano activity, such as well graded sand (SW), well-graded silty sand (SW-SM), silty sand (SM) and poorly graded sand (SP); Capilleri and Massimino [7] studies gravelly-sandy nature with a variability of particle size being classified as SP and SW; Bandini et al. [4] as poorly graded sand (SP).

The evaluation of specific gravity of solid particles (G_s) by water pycnometer is performed by [15] and natural water content (w_n) is determined by [14], as summarized in Table 7. The value of G_s is also determined for the CS sample for the confirmation of the study by the application of gas pycnometer according to [15], resulting in $G_s = 2.852$, thus being considered valid as obtained of the similar order as deduced by water pycnometer and confirming the analysis for other samples.

The G_s value of VA samples from the island of La Palma deposited in 2021 and studied for this paper ranges from 2.71 to 3.04, being greater than the other values of G_s published worldwide for other VA and typical ordinary sand samples such as Toyoura sand. The range of G_s values for Japanese VA ranges from 2.56 from Naganuma, 2.47 at Aratozawa, 2.82 in Mori as summarized in Liu et al. [31]; for Japanese VA from 2.63 to 2.83 [39]; for Etna VA from 2.5 to 2.7 [7]; for Iranese VA ranges from 2.57 to 2.64 [3]; for VA from Papua New Guinea 2.45 [22]), for VA from Mashhad in Iran 2.05 [48]; and for conventional Toyoura sand is 2.65 [39,31]. More extensive summary of G_s values is given in Jativa et al. [26] for worldwide deposited VA providing wide range from 2.08 to 3.04.

Compaction

Compaction tests were performed to determine relation of water

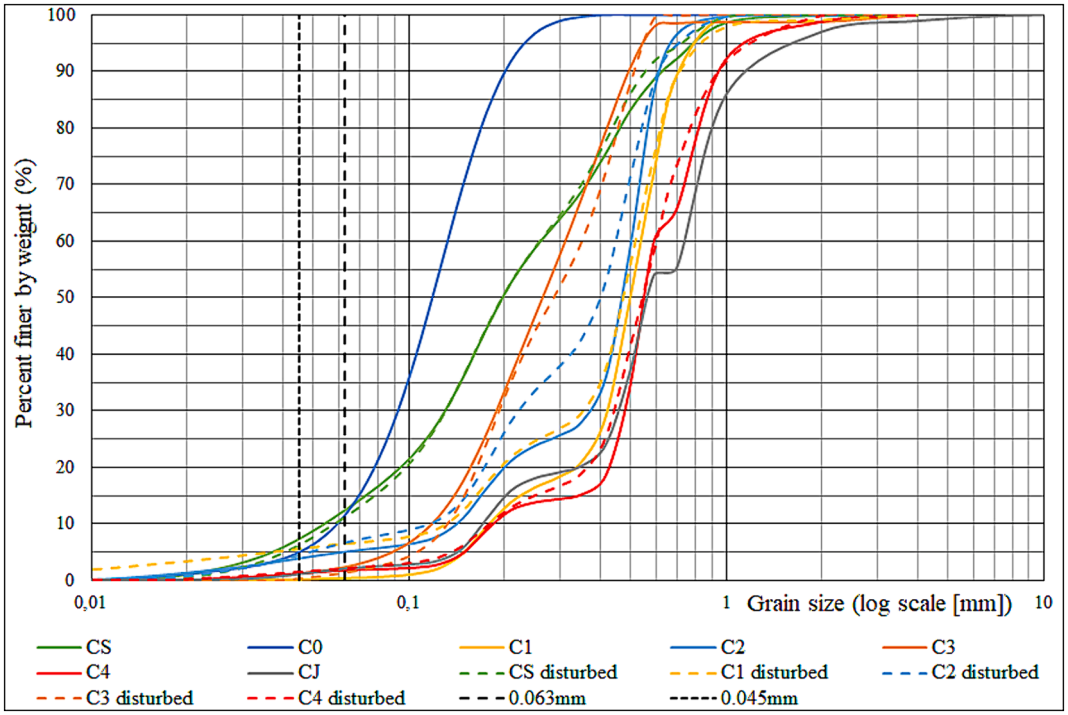

Fig. 4. Grain size distribution curve of VA samples.

Table 6
Grading and soil classification according to USCS of samples.

Sample	% > 2 mm	% < 2 mm	% > 700 μm	% < 700 μm	Fines content (<63 μm) (%)	D_{60} (mm)	D_{30} (mm)	D_{10} (mm)	C_u	C_z*	USCS
C0	0.0	100.0	0.0	100.0	11.7	0.13	0.09	0.06	2.31	1.09	SP
CS	1.3	98.8	11.4	88.6	12.5	0.26	0.13	0.05	4.87	1.20	SP
C1	1.3	98.8	27.9	72.1	0.3	0.54	0.42	0.18	2.97	1.82	SP
C2	0.2	99.8	13.8	86.3	5.0	0.51	0.37	0.14	3.77	1.93	SP
C3	1.3	98.7	2.2	97.8	2.3	0.31	0.19	0.11	2.78	1.01	SP
C4	1.1	98.9	40.1	59.9	1.7	0.59	0.48	0.18	3.18	2.05	SP
CJ	2.9	97.1	46.0	54.0	2.0	0.63	0.45	0.17	3.67	1.86	SP

* Cz: coefficient of gradation

Table 7
Specific gravity of solid particles and natural water content.

Sample	G_s (water pycnometer)	w_n (%)
CS	2.884	0.1
C1	3.042	3.9
C2	3.034	5.9
C3	2.970	3.1
C4	2.959	2.2
CJ	2.714	–

content and dry unit weight for each VA sample based on Standard Proctor test with the compaction energy by a 2.5 kg hammer dropped from 30 cm height over the soil in the mold of 101.6 mm diameter (UNE 103–500). In this case the standard compaction energy is used considering that low difference is expected being the material poorly graded, being considered that the compaction energy would have limited low effect on this material [12]. Fig. 5 shows the compaction and zero void curves, while the values of maximum dry unit weight and optimum water content are summarized in Table 8. The values of void ratio obtained for the Proctor test are also included, determined for the maximum dry unit weight and G_s.

Considering low values of uniformity coefficient (C_u) for uniformly graded soils, VA are classified as poorly compactable, that is confirmed by difficulties in performing the compaction, as can be seen the

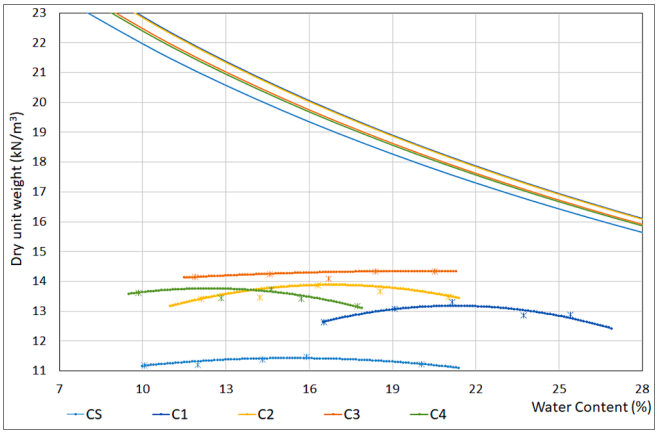

Fig. 5. Compaction curves and zero void curves of VA samples.

compaction curves having low amplitude in dry unit weight for all studied VA samples, being void spaces between particles hard to fill due to almost the same size of voids. The lowest dry specific weight is obtained for sample CS in the order of 11.5 kN/m^3, attributed to high % of fines content. The samples C1 through C4 have dry unit weight in the range of 13.5 and 14.5 kN/m^3 with quite variable optimal water content

Table 8
Summary of compaction tests: unit dry weight and optimum water content.

Sample	γ_{dmax} (kN/m^3)	W_{opt} (%)	e (Proctor)
CS	11.4	15.4	1.48
C1	13.2	21.3	1.26
C2	13.8	16.7	1.16
C3	14.3	20.0	1.03
C4	13.8	12.4	1.11

ranging from 12 to 20 %. It can also be observed the zero void curve having great difference in comparison to the compaction curves. Other studies of VA present greater variability in the compaction curves being defined in the range of poorly to well graded sandy material [39].

The minimum and maximum unit dry weight (γ_{dmin} and γ_{dmax}) of VA is also determined, only performed for the sample CS according to standards UNE 103–105 (pouring VA through a funnel to a specific mold) and [58] (applying the ramming method), respectively. It is observed a great amplitude in values of minimum and maximum unit dry weight ranging from 8.5 to 14.1 kN/m^3 corresponding to its densest and loosest state. These values are further used as reference values to define the relative density of CS sample in the one-dimensional consolidation and collapse test (see chapter 4.4 and 4.5).

One-dimensional consolidation test

From gradation curves can be seen that all curves contain more than 97 % of sandy material (<2 mm). The material was selected passing through 2 mm sieve for the analysis of deformation characteristics by one-dimensional consolidation test. All samples were subjected to one-dimensional consolidation testing in order to evaluate deformation properties, and are tested in the mold of the circular section of 70 mm diameter and height of 20 mm. To ensure uniform specimens to be tested, the dry material was poured into the metal mold through a funnel with zero drop simulating natural loose state. After the specimen preparation, it was inundated and the stage loading is applied according to [17]. Different constant vertical loads were applied till consolidation was finished, applying load stages of 10, 20, 40, 80, 150, 300, 600, 1000, 1500 kPa every 24 h, and consequently unloading the specimen in four stages (1000, 300, 40, 10 kPa every 24 h). Following Fig. 6 shows different relationships obtained: (a) specimen vertical deformation vs time for each load step applied, (b) specimen vertical deformation (%) vs applied load (log(σ_v')), (c) void ratio (e_i/e_0) vs applied load (log(σ_v')), and (d) deformation modulus vs applied load (log(σ_v')) at different vertical applied load step.

It can be observed from Fig. 6 different volumetric deformation behavior being different range of strains obtained for each specimen under consolidation test, being the lowest deformation of approximately 3 % observed for the specimen C3 while the greatest up to 11.5 to 12.5 % observed for specimen CS and CJ, respectively. This is due to different gradation size of specimens, being greater for larger range of grain size for different samples. Studies conducted by Capilleri and Massimino [7] reported greater strain ranges from 2 to 47.5 %. Also, there is a difference in the range of deformation modulus observed depending on the grain size distribution and mineralogy. In general, for all specimens, the unloading part of curves (see Fig. 6b,c) present small deformation recovery in comparison to the plastic unrecovered strains, being this behavior typical for sandy materials also resulting in low range of unloading modulus for different specimens.

Table 9 presents the summary of different deformational parameters

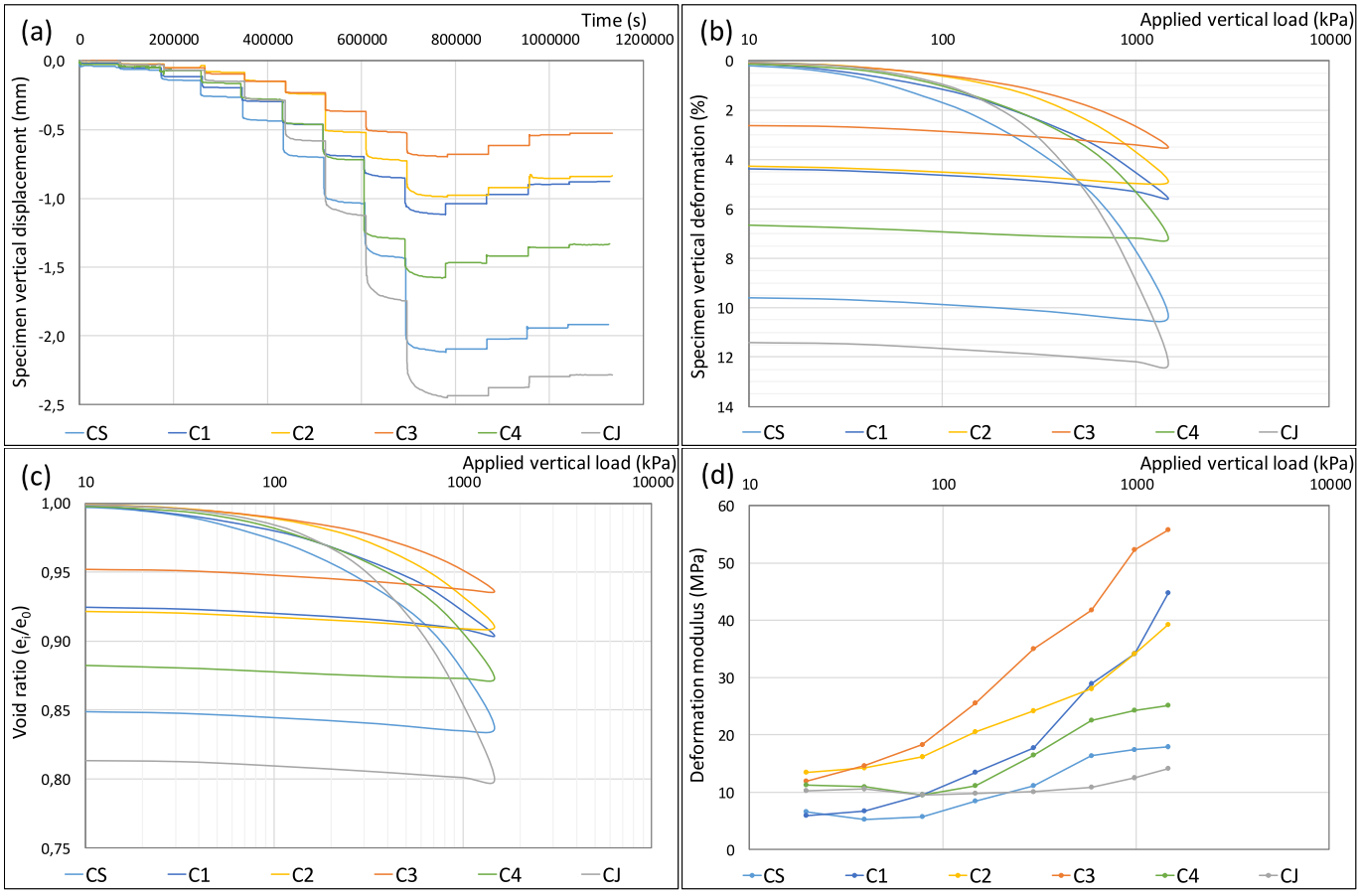

Fig. 6. One-dimensional consolidation tests: (a) vertical displacement vs time, (b) vertical deformation (%) vs load, (c)void ratio (e_i/e_0) vs load, (d) deformation modulus vs load.

Table 9
Summary of deformation modulus, compression and recompression index, void ratios and water content during one-dimensional consolidation test.

Specimen	E_{oedo}* (MPa)	E_{ur}* (MPa)	C_c	C_r	e_i	e_f	Δe (%)	Water content final (%)
CS	17.6	55.6	0.22	0.016	1.74	1.47	15.10	44.6
C1	39.4	59.2	0.12	0.015	1.38	1.28	7.56	39.1
C2	36.7	68.2	0.14	0.008	1.21	1.11	7.82	30.4
C3	54.0	63.0	0.11	0.009	1.20	1.14	4.78	32.4
C4	24.7	66.0	0.18	0.006	1.31	1.16	11.74	31.1
CJ	13.3	61.7	0.36	0.013	1.58	1.28	18.65	40.0

* E_{oedo} and E_{ur}: deformation modulus under loading and unloading conditions.

deduced from one-dimensional consolidation tests, i.e. deformation modulus under loading (E_{oedo}) determined as the slope of the ε-logσ' curve for the final loading stage up to 1500 kPa and modulus under unloading conditions (E_{ur}) determined as the slope of the unloading part of the ε-logσ' curve being considered as a straight line, reaching the range of values 20–40 MPa and 50–60 MPa, respectively. The compression (C_c) index is determined as the slope of the linear portion of e-logσ' curve and recompression (C_s) index for the expansion part of e-logσ' curve being approximated to a straight line, reaching range of values from 0.1 to 0.2 and 0.01 to 0.015, respectively. There is a greater difference between the range of deformation modulus under loading, while the unloading path has negligible difference for different tested specimens. The relation between E_{oedo} and E_{ur} ranges between 1.5 and 3 while the relation of C_c and C_s is between 0.1 and 0.15.

Table 9 also summarizes results of the void ratio of the material at the beginning (e_i) and at the end (e_f) of the one-dimensional consolidation test, as well as the water content at the end of the one-dimensional consolidation test being considered as water absorption. It can be observed the very small reduction of void ratio (Δe) in general being in the range of 4.8 to 18.7 %, corresponding the lowest reduction to C3 and the greatest to CJ and CS. The final water content ranges from 30 to 45 % for different specimens, corresponding the greatest to CJ and CS, and the lowest to C2, C3 and C4.

It can be observed in Fig. 6 that the greatest decrease in the specimen height, i.e. greatest deformation, greatest void ratio and lowest deformation modulus under loading conditions is observed for the specimen CS (see Table 9). The range of initial void ratios can be observed for different VA specimens tested. As previously stated in chapter 4.3, for the specimen CS, the minimum and maximum dry unit weight is determined (8.5 and 14.1 kN/m^3), and compared to the dry unit weight observed at the beginning and at the end ($\gamma_{d,initial}$ and $\gamma_{d,final}$) of the one-dimensional consolidation test, being the relative density determined in the range of 44 to 64 % for the applied load range up to 1500 kPa (Table 10). The values of $\gamma_{d,initial}$ and $\gamma_{d,final}$ are simply obtained by the weight of dry material in the mold poured at the beginning and after the performance of one-dimensional consolidation test.

Collapse test

The one-dimensional collapse tests were performed in consolidometer over specimens CS, C1, C2, C3, C4 and CJ following UNE 103–406 standard up to the load of 200 kPa. The dry material was poured into the cylindrical metal mold (diameter of 70 mm and height 20 mm) through a funnel with zero drop simulating natural loose state in order to perform the test in consolidometer. After the initially applied seating load of 5 kPa, the load is applied every 1 h over the dry material at different load steps (12, 25, 50, 100 and 200 kPa). 1 h after the application of the load of 200 kPa, the specimen was inundated maintaining the load during next 12 h considering that by that time the stabilization of the settlement curve is reached. After that, the load is applied up to 400 and 800 kPa during 12 h each step, and consequently completely unloaded. Fig. 7 presents the relation of specimen vertical deformation and applied vertical load. The collapse index (I_e) is determined by the measurement of the collapse as height reduction after the introduction of the distilled water 1 h after the application of maximum load of 200 kPa in the consolidometer (UNE 103–406). The value of I_e determined at stress level of 200 kPa ranges from 0.1 to 0.4 % for each specimen (Table 11 and Fig. 7), being these values very low and considered as slight values in terms of collapse index. This procedure of the collapse test was also performed over specimens C2, C3 and C4 up to a greater load being the specimen inundated reaching 400 kPa (stages at 12, 25, 50, 100, 200 and 400 kPa), and the collapse index estimated from 0.1 to 0.2 % at stress level of 400 kPa.

Table 10
Summary of maximum and minimum density for CS for one-dimensional consolidation test.

Sample	γ_{dmax} (kN/m^3)	γ_{dmin} (kN/m^3)	$\gamma_{d,initial}$ (kN/m^3)	$\gamma_{d,final}$ (kN/m^3)	$D_{r,initial}$ (%)	$D_{r,final}$ (%)
CS	14.1	8.5	10.3	11.4	43.9	64.2

Table 11 summarizes the collapse index, void ratio at the beginning (e_i) and at the end (e_f) of the collapse test, and the final water content. It can be observed the very small reduction in void ratio (Δe), in the similar trend as for one-dimensional consolidation test, varying from 2.8 to 12.9 % for the maximum load applied up to 800 and 400 kPa, corresponding the lowest to specimen C3 and the highest to specimens CS and CJ. The final water content ranges from 30 to 46 % for different VA specimens, being the lowest related to C3, C2 and C4, while the greatest correspond to CS and CJ, being of the same order as can be observed for VA specimens tested in one-dimensional consolidation test.

As previously determined for the specimen CS in chapter 4.4 regarding the relative density at the beginning and at the end of the one-dimensional consolidation test, the relative density is determined for the sample CS before and after the collapse test ranging from 44 to 60 % (Table 12) for the applied load up to 800 kPa, being of the same order as obtained for one-dimensional consolidation test.

Direct shear test

Direct shear tests were performed on all VA samples in order to evaluate shear strength properties according to [18]. The specimens were tested in the square mold of the section of 36.0 cm^2 and initial height of 3.0 cm. The material was poured into the shear box apparatus through a funnel with zero drop simulating natural loose state. After specimen preparation, different constant consolidation normal stress is applied after specimen inundation (ranging from 50 to 300 kPa) for 24 h till consolidation is finished and prior to the application of the shear stress, being these normal stresses maintained constant during the shear phase of the test. The displacement velocity adopted during the failure phase of the test for the application of the shear stress along the prescribed failure surface was 0.03 mm/min.

Fig. 8 summarizes the relation between the shear stress and the horizontal displacement under different normal stresses (50, 100, 200 and 300 kPa) for tested specimens (VA sample C1, C2, C3 and C4). As expected, the increase in shear strength is observed with increasing normal stress. It can be observed that the lower the normal stress, the peak value of shear stress is obtained for smaller horizontal deformation. Fig. 10 presents the shear stress envelope for different VA specimens tested, deduced from Fig. 8 for peak values of the shear strength. It can

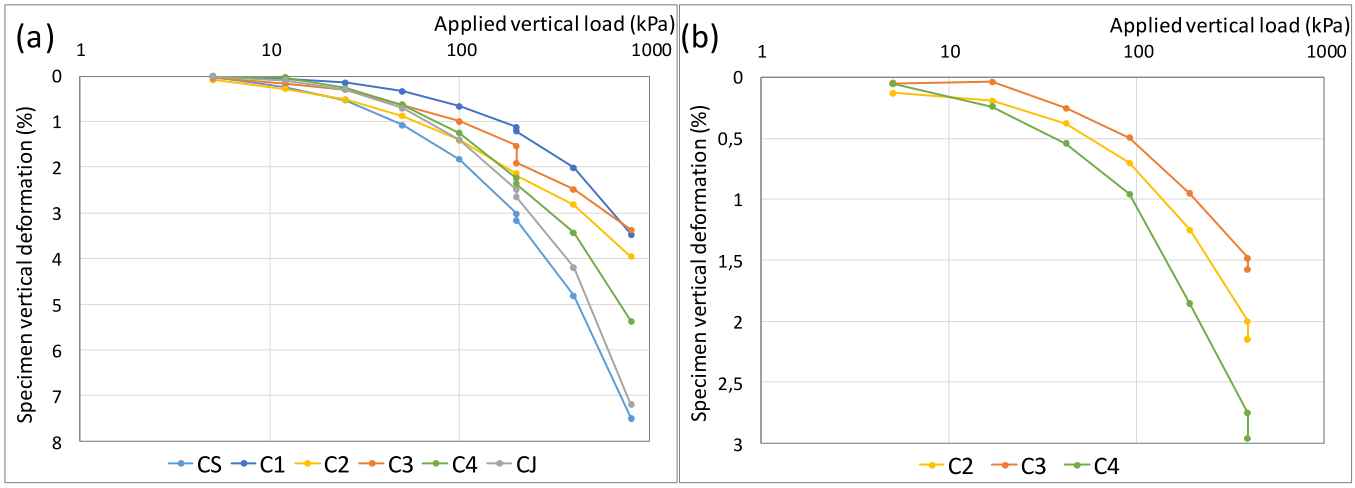

Fig. 7. Specimen vertical deformation vs applied load for inundation at (a) 200 kPa and (b) 400 kPa.

Table 11
Summary of collapse index, void ratios and water content during collapse test.

Specimen	Inundation load (kPa)	I_e (%)	e_i	e_f	Δe (%)	Water content final (%)
CS	200	0.15	1.74	1.53	11.8	45.9
C1	200	0.09	1.35	1.27	6.1	37.4
C2	200	0.05	1.20	1.12	7.3	30.3
C3	200	0.37	1.17	1.11	5.3	34.6
C4	200	0.13	1.43	1.30	9.1	32.2
CJ	200	0.17	1.26	1.10	12.9	41.5
C2	400	0.15	1.29	1.24	3.8	33.1
C3	400	0.10	1.22	1.23	2.8	32.2
C4	400	0.21	1.36	1.35	5.1	31.5

Table 12
Summary of maximum and minimum density for CS for collapse test.

Sample	γ_{dmax} (kN/m^3)	γ_{dmin} (kN/m^3)	$\gamma_{d,initial}$ (kN/m^3)	$\gamma_{d,final}$ (kN/m^3)	$D_{r,initial}$ (%)	$D_{r,final}$ (%)
CS	14.1	8.5	10.3	11.2	44.1	59.9

be observed the similar values for all studied specimens, being the variation of friction angle from 30° to 34°, typical of the loose state of clean sandy material, as summarized in Table 13. These values are in the range of values (29 to 34°) provided by Capilleri and Massimino [7]. For some of the failure curves, it can be observed a light curvature in the relation of normal and shear stress.

Fig. 9 represents the correlation between the vertical and horizontal displacement during failure stage obtained for all VA specimens under different normal stress. As expected, being VA of this study the sandy soils in its loose state, the expected clear dilation behavior can be observed for all samples, being greater for lower normal stress applied. The results presented in Fig. 9 are summarized in Table 13, resulting in important dilation of all tested specimens, that is defined as a property of a granular soil representing a change in its volume in response to shearing stress under certain normal stress, corresponding to following medium values of 9.5°, 7.5°, 6.5° and 5.5° under different normal stress of 50, 100, 200 and 300 kPa, respectively. Table 13 summarizes average values of dilation angle for each VA sample material for the range of applied normal stresses, for studied VA specimens. The lower negligible values of dilation angle ranging from 0 to 4° are obtained by Capilleri and Massimino [7].

Table 14 presents the summary of void ratio of the material at the beginning and at the end of the direct shear test, being the final reduction in void ratio from 2.8 to 27.3 %, being the lowest reduction observed for C3 and the greatest for C4 specimen. Also, the water content evaluated at the end of the direct shear test, considering that the material was set in completely dry state introduced in the mold, presenting at the end of the test the water content range from 32 to 37 %, corresponding the lowest to C4 and the greatest to C1, and being of the same order as presented for one-dimensional consolidation test (Table 9) and collapse test (Table 11).

Particle crushing evaluation

Particle crushing for the study of the integrity of particles is evaluated by analyzing grain size distribution curves after the performance of one-dimensional consolidation tests in order to compare it to the ones obtained on the natural material prior to subject it to loading process, being considered its possible change in its granulometry due to compaction of material inducing particle friction. In order to quantify the particle crushing, the relationship given by Lade et al. [28] and Miura et al. [38] is used. The definition of Lade et al. [28] considers particle crushing parameter $B_{10} = 1\text{-}D_{10f}/D_{10i}$, being D_{10i} the initial effective grain size prior to loading and D_{10f} the final effective grain size after performance of either direct shear or one-dimensional consolidation test. The criterion proposed by Miura et al. [38] considers the increment in fines content due to application of loading in one-dimensional consolidation test.

Table 15 summarizes the analysis of grain size distribution curves of disturbed curves after the performance of one-dimensional consolidation tests. The distribution curves of disturbed samples are presented in Fig. 4 in conjunction with samples in natural state prior to performance of different tests for its comparison. A variability in gradation curves can be observed as for undisturbed samples prior to testing being all defined as poorly graded sand (SP) according to UCSC classification system, based on values of C_u in the range of 2.7 to 4.5, and C_z ranging from 0.8 to 1.9, with fines content within 2.2 and 14.3 %. The increase of fines content can be observed in the majority of studied VA samples, or similar to previously determined granulometry in natural state, being attributed to variability of the particle size distribution of VA samples.

Table 16 summarizes the analysis of the crushing according to Lade et al. [28] and Miura et al. [38]. The crushing defined by previously mentioned 2 methods are indicating variability in particle size crushing depending on the sample, being the lowest for CS, C4 and C3, and the greatest for samples C1 and C2. Anyway, from Fig. 4 can be observed that some of the gradation curves are similar for the state prior to and after the test, such as samples CS and C3. Other samples, such as C1, C2 and C4, showing small gap-graded nature in the fraction from 0.2 to 0.4 mm in its natural state, show the greatest difference in the shape of the

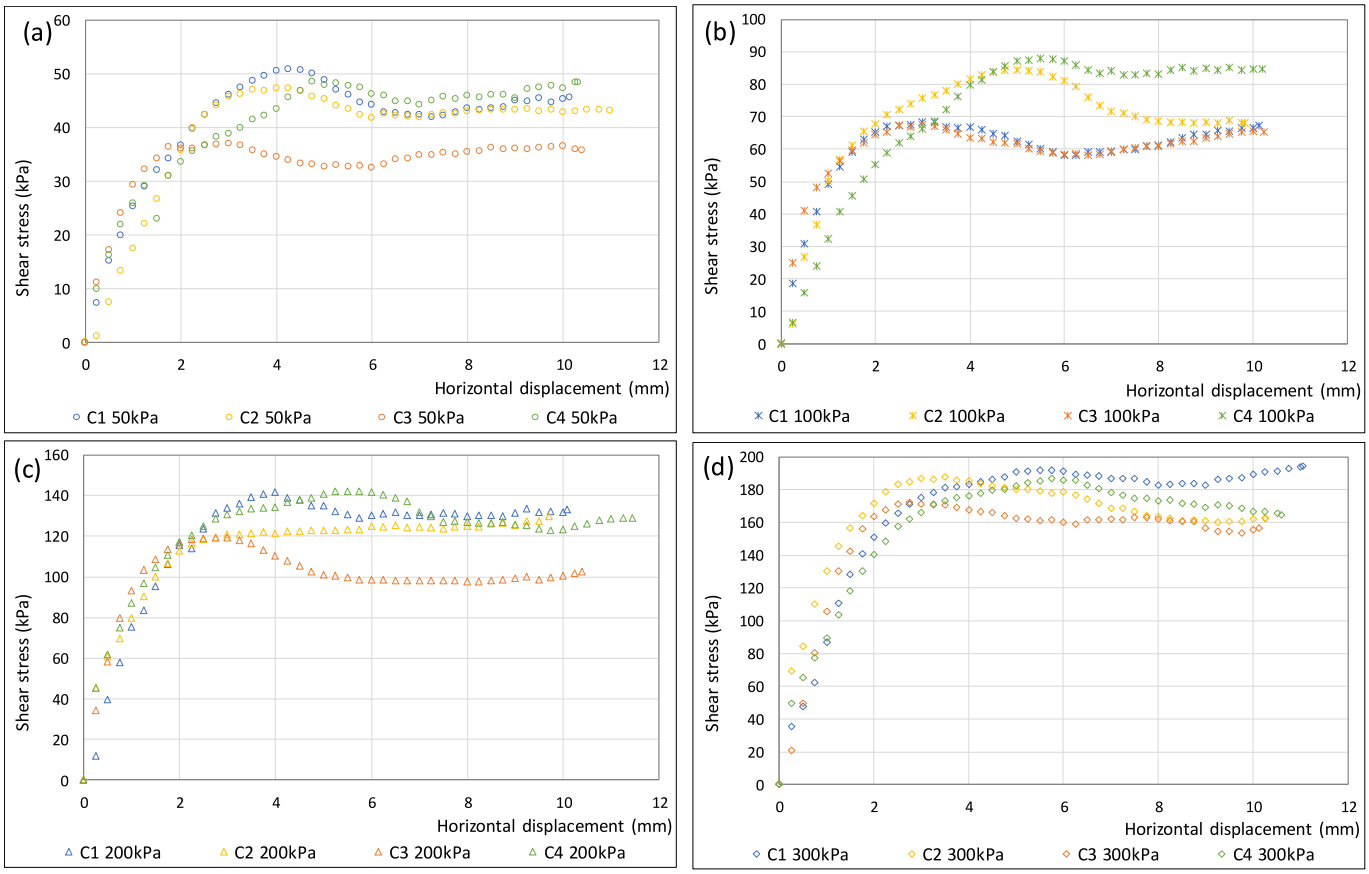

Fig. 8. Shear stress vs. horizontal displacement during failure stage under different normal stress (50, 100, 200 and 300 kPa).

Table 13
Resistance parameters of tested VA specimens.

Sample	Friction angle (°)	Dilation angle (°)
C1	33.5	7
C2	33.0	6
C3	30.5	9
C4	34.0	7

gradation curve being the content of the missing fraction increased after the test. The increase of the fines content particle size fraction is variable, presenting in general the variability from 0.5 to 2.2 %, except for sample C1 reaching 6.4 %.

Discussion and conclusions

The increasing activity in volcano eruptions is observed worldwide. In this case, the volcanic ash from La Palma island is studied, being this the most frequently active volcano of Canary Islands, Spain, causing great problems for the population. This material is of increasing interest worldwide due to its possibility for the use as resource material. The summary and discussion of mineralogical, chemical and geotechnical properties, analyzed under static conditions, is the following:

- This VA is of a sandy nature, being classified as poorly graded.
- According to the chemical analysis, this VA contains $SiO_2 + Al_2O_3 + Fe_2O_3$ up to the range from 65 to 70 %, being close to the limit value for its classification as class N or class F pozzolans (ASTM C618). The relation $SiO_2/Al_2O_3 < 3.9$ indicates its suitability for geopolymer, but the low amorphous phase < 36 % does not indicate its suitability for alkali-activation. Thus, the necessity of its activation by adding mineral additives such as lime, metakaolin, granulated blast furnace slag, fly ash, should be considered to compensate the content of SiO_2, Al_2O_3 and CaO.
- Values of pH indicates the necessity for its increase by the addition of additive to reach the required value for its use as geopolymer. Values of electrical conductivity are low indicating low presence of soluble salts.
- The compaction tests present low amplitude in the unit dry weight for the range of water content due to its poor gradation curve, being extremely difficult its compaction and considered the standard method of compaction as not applicable for these materials.
- The deformation and resistance parameters of studied volcanic ashes have similar patterns as of sandy soils.
- The one-dimensional consolidation testing indicates different range of settlements, depending on the particle size distribution and mineralogy composition, ranging from 3 to 12.5 % of the specimen height.
- The deformational modulus determined in one-dimensional consolidation tests varies for different samples collected on different locations, depending on the grain size distribution and mineralogy, being in the range of 20 to 40 MPa for the maximum loading stage corresponding to 1000 to 1500 kPa, thus considered in general very low as a direct foundation for any construction on these material.
- The unloading deformation modulus has little difference for different samples, in the order of 50 to 60 MPa, presenting small deformation recovery in comparison to the plastic unrecovered strains, being this behavior typical for sandy materials.
- The collapse test shows negligible values of the collapse index.
- The direct shear test shows similar results for different samples regarding values of friction angle (ranging from 30 to 34°), corresponding the lowest value to sample of the most uniformly

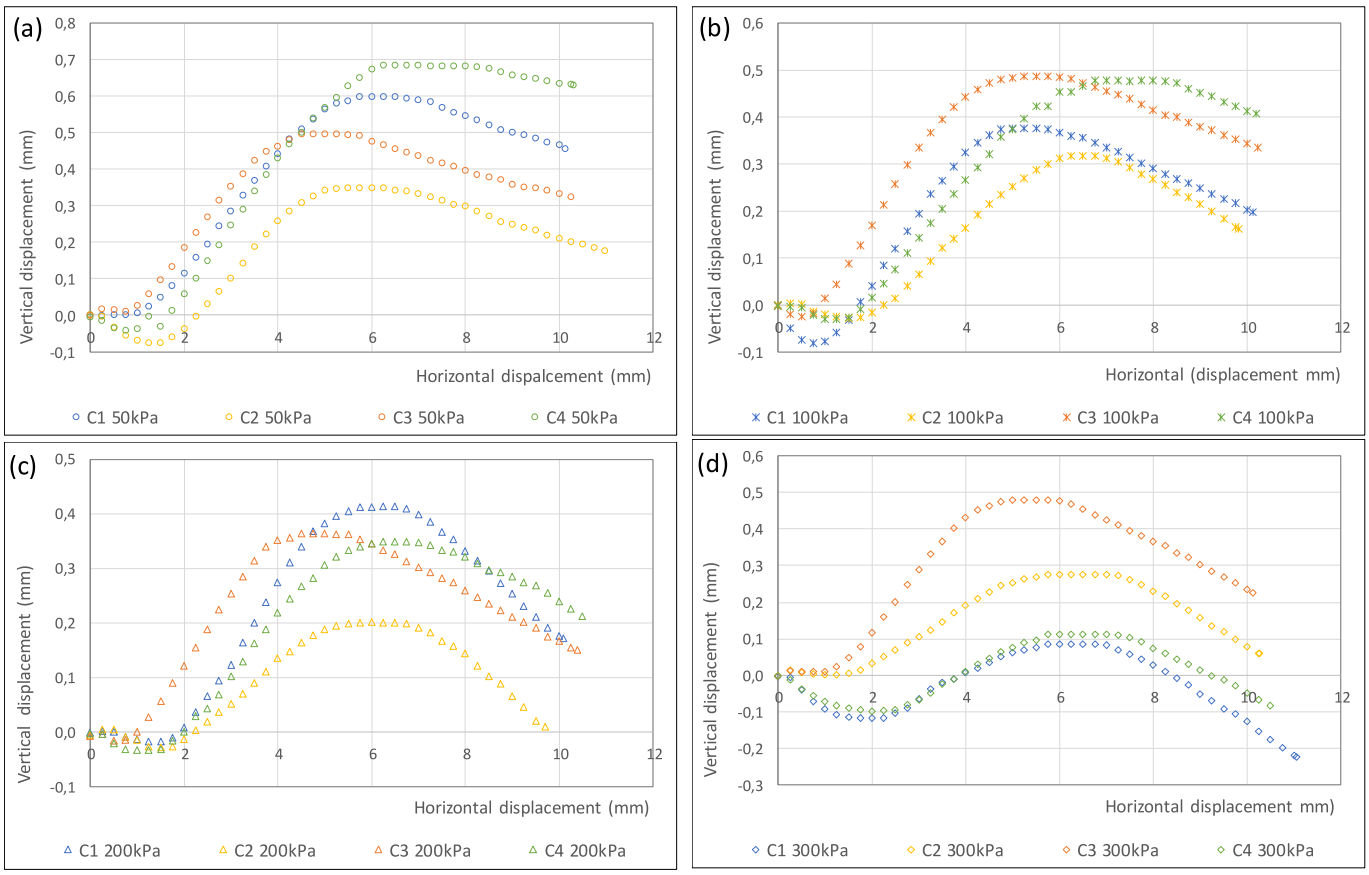

Fig. 9. Vertical vs. horizontal displacement during failure stage under different normal stress (50, 100, 200 and 300 kPa).

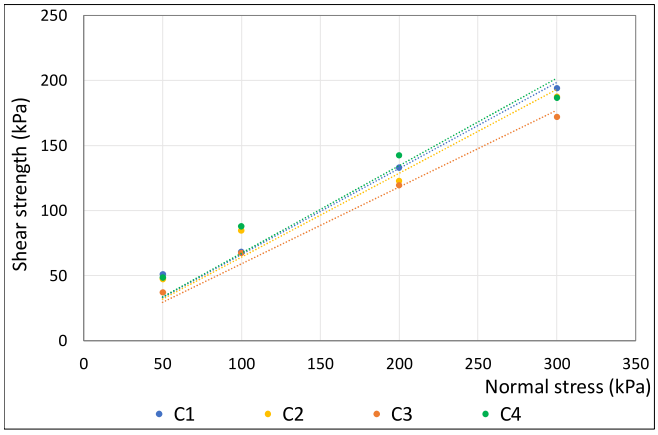

Fig. 10. Failure envelope for different VA specimens.

Table 14
Summary of void ratios and water content during direct shear test.

Specimen	e_{ic}	e_{fc}	e_f	Δe (%)	Water content final (%)
C1	1.31	1.28	1.14	14.5	36.8
C2	1.27	1.26	1.04	22.0	34.3
C3	1.06	1.04	1.03	2.8	34.6
C4	1.25	1.21	0.98	27.3	32.1

distributed grain size. These values of friction angle are considered low corresponding to loose clean sandy material and by that way could be considered of the same nature, not depending on the location after emission of VA during eruption.

- The volumetric change is observed during performance of direct shear tests, evaluated by dilation angle range from 5 to 10°, typical for material of sandy nature in its loose state, being the highest value observed for low confining pressure and the lowest for high confining pressure.
- The relative density determined at the beginning and at the end of one-dimensional consolidation and collapse test for the sample CS indicates 44 % in the loosest state up to 60–64 % depending on the static load applied, being considered as low improvement of the relative density by static methods.
- The variation of the void ratio at the beginning and at the end of the one-dimensional consolidation and collapse test indicates the range between 3 to 19 %, while for the direct shear test this range in the order of 3 to 27 %, depending on the applied static load, and being considered as low compaction improvement by static methods.
- Particle crushing is determined for samples after performance of one-dimensional consolidation tests, presenting variability regarding the change in the particle size distribution for different particle sizes. The gap-graded samples show the increase of the missing fraction content after the performed test.
- Based on performed static loading tests, i.e. one-dimensional consolidation, collapse and direct shear test, the water absorption is evaluated based on the final water content measured in the range from 30 to 50 %, as expected due to its high porosity.

The following main conclusions of the study can be made:

- The general geotechnical behavior of fresh VA is typical for loose poorly graded sandy soils.
- The studied engineering properties of different VA samples, vary depending on the collection point with respect to the location from the emission source of the volcano activity and time of the collection

Table 15
Grading and soil classification according to USCS of disturbed samples.

Sample	% > 2 mm	% < 2 mm	% < 700 μm	% > 700 μm	Fines content (<63 μm) (%)	D_{60} (mm)	D_{30} (mm)	D_{10} (mm)	C_U	C_Z	USCS
CS disturbed	0	100	8.2	91.9	11.3	0.26	0.13	0.06	4.51	1.12	SP
C1 disturbed	1.2	99.0	25.2	74.8	6.4	0.52	0.36	0.13	4.04	1.87	SP
C2 disturbed	0.4	99.6	12.1	87.9	6.8	0.45	0.23	0.11	4.17	1.05	SP
C3 disturbed	0.2	99.8	0.8	99.2	1.5	0.34	0.20	0.13	2.73	0.82	SP
C4 disturbed	1.3	98.7	41.9	58.1	2.1	0.60	0.44	0.18	3.41	1.81	SP

Table 16
Particle crushing evaluated by different methods.

Sample	Lade et al. [28]	Miura et al. [38]
CS	0.078	1.220
C1	0.941	6.394
C2	0.406	2.219
C3	0.332	1.110
C4	0.290	0.535

after the volcano eruption, thus influencing the mineralogical and chemical composition, and consequently affecting its compaction, strength and deformation characteristics.

- The studied VA does not have suitable geotechnical properties to be used in its natural state as the base of roads, embankment material, foundation of geotechnical structures, etc., considering difficulties in its compaction by standard methods, low deformation modulus and resistance parameters. Potential future uses should be considered for its recovery for the production of cement, mortar, asphalt, ceramics, bricks, etc., as well as for soil stabilization.
- The engineering properties of this VA in fresh state could be considered as general values, but should not be extrapolated for other VA considering possible differences in chemical composition.

Author statement

This work has not been supported by any external funding, only the internal by the Faculty of Geology (UCM) (Madrid, Spain). The AEMC15/22–30121 grant of Acciones Especiales de Investigación 2022 of UCM is acknowledged. The UCM Research Group 520, Crystallographic and Geological techniques. Non-Conventional Applications, is also acknowledged.

CRediT authorship contribution statement

Svetlana Melentijević: Writing – original draft, Visualization, Resources, Project administration, Methodology, Investigation, Formal analysis, Data curation, Conceptualization. **Sol López-Andrés:** Writing – review & editing, Visualization, Validation, Supervision, Resources, Project administration, Investigation, Conceptualization. **José Estaire:** Writing – review & editing, Validation, Supervision, Conceptualization.

Declaration of competing interest

The authors declare that they have no known competing financial interests or personal relationships that could have appeared to influence the work reported in this paper.

Data availability

Data will be made available on request.

Acknowledgements

The authors are grateful to Professor Eumenio Ancochea, and the students and Professors of the Master of Environmental Geology at UCM for collecting and shipping the material to the Faculty of Geology (UCM) and to the Geological Techniques Unit Laboratory (Research Assistance Centre of Earth Sciences and Archaeometry, UCM).

References

[1] Alraddadi S, Assaedi H. Characterization and potential applications of different powder volcanic ash. J King Saud University Science 2020;32:2969–75. https://doi.org/10.1016/j.jksus.2020.07.019.
[2] American Coal Ash Association 2003. Fly ash facts for highway engineers, Technical Report No. FHWA-IF-03-019, FHWA, USA.
[3] Bahadori H, Hasheminezhad A, Taghizadeh F. 2019. Experimental study on marl soil stabilization using natural pozzolans. J. Mater. Civ. Eng. ASCE 31(2): 04018363. https://doi: 10.1061/(ASCE)MT.1943-5533.0002577.
[4] Bandini V, Biondi G, Cascone E, Di Filippo G. Dynamic image analysis of Etna Sand in one-dimensional compression. Measurement 2017;104:336–46. https://doi.org/10.1016/j.measurement.2016.07.050.
[5] Barone G, Finocchiaro C, Lancellotti I, Leonelli C, Mazzoleni P, Sgarlata C, et al. Potentiality of the use of pyroclastic volcanic residues in the production of alkali activated material. Waste Biomass Valoriz 2021;12:1075–94. https://doi.org/10.1007/s12649-020-01004-6.
[6] Belfiore CM, Amato C, Pezzino A, Viccaro M. An end of waste alternative for volcanic ash: a resource in the manufacture of ceramic tiles. Constr Building Mat 2020;263(1–15):120118.
[7] Capilleri PP, Massimino MR. Geotechnical characterization of ash collected during recent eruptions of Mount Etna: from dangerous waste material to environmental friendly resource. Geomech Geophys Geo-energ Geo-resour 2019;5:383–403. https://doi.org/10.1007/s40948-019-00119-y.
[8] Carracedo JC, Troll VR, Day JM, Geiger H, Aulinas M, Soler V, et al. The 2021 eruption of the Cumbre Vieja volcanic ridge on La Palma. Canary Islands Geology Today 2022;38(3):94–107. https://doi.org/10.1111/gto.12388.
[9] Contrafatto L. Recycled Etna Volcanic ash for cement, mortar and concrete manufacturing. Constr Building Mat 2017;151:704–13.
[10] Cultrone G. The use of Mount Etna volcanic ash in the production of bricks with good physical-mechanical performance: Converting a problematic waste product into a resource for the construction industry. Ceramics Int 2021. https://doi.org/10.1016/j.ceramint.2021.11.119.
[11] EN 13038: 2012. Soil improvers and growing media. Determination of electrical conductivity.
[12] EN 16907-1:2018. Earthworks Part 1: Principles and General Rules.
[13] EN 17693-1: 2022. Earthworks. Soil treatment tests. Part 1: pH-test for determination of the lime requirement of soils for stabilization (Lime Fixation Point LFP, Lime Modification Optimum LMO).
[14] EN ISO 17892-1: 2015. Geotechnical investigation and testing - Laboratory testing of soil - Part 1: Determination of water content.
[15] EN ISO 17892-3: 2018. Geotechnical investigation and testing - Laboratory testing of soil - Part 3: Determination of particle density.
[16] EN ISO 17892-4: 2019. Geotechnical investigation and testing - Laboratory testing of soil - Part 4: Determination of particle size distribution.
[17] EN ISO 17892-5: 2019. Geotechnical investigation and testing - Laboratory testing of soil - Part 5: Incremental loading oedometer test.
[18] EN ISO 17892-10: 2019. Geotechnical investigation and testing - Laboratory testing of soil - Part 10: Direct shear tests.
[19] Finocchiaro C, Barone G, Mazzoleni P, Leonelli C, Gharzouni A, Rossignol S. 2020. FT-IR study of early stages of alkali activated materials based on pyroclastic deposits (Mt. Etna, Sicily, Italy) using two different alkaline solutions. Constr. Building Mat. 262:1–11:120095.
[20] Ghadir P, Zamanian M, Mahbubi-Motlagh N, Saberian M, Li J, Ranjbar N. Shear Strength and Life Cycle Assessment of Volcanic Ash-based geoplymer and Cement Stabilized Soil: A Comparative Study. Trans Geotech 2021;31:100639. https://doi.org/10.1016/j.trgeo.2021.100639.
[21] Ghadir P, Ranjbar N. Clayey soil stabilization using geopolymer and Portland cement. Constr Building Mat 2018;188:361–71.
[22] Hossain KMA, Mol L. Some engineering properties of stabilized clayey soils incorporating natural pozzolans and industrial wastes. Constr Building Mat 2011; 25:3495–501. https://doi:10.1016/j.conbuildmat.2011.03.042.
[23] Hurlimann M, Ledesma A, Martı J. Characterisation of a volcanic residual soil and its implications for large landslide phenomena: application to Tenerife, Canary Islands. Eng Geol 2001;59:115–32. https://doi.org/10.1016/S0013-7952(00)00069-7.
[24] International Volcanic Health Hazard Network, IVHHN. https://www.ivhhn.org/index.php/guidelines#ash-collection.

[25] ISO 13320:2020(E). Particle size analysis – laser diffraction methods.
[26] Jativa A, Ruales E, Etxeberria M. Volcanic Ash as a Sustainable Binder Material: An Extensive Review. Materials 2021;14:1302. https://doi.org/10.3390/ma14051302.
[27] Khan K, Amin MN, Saleem MU, Qureshi HJ, Al-Faiad MA, Qadir MG. Effect of Fineness of Basaltic Volcanic Ash on Pozzolanic Reactivity, ASR Expansion and Drying Shrinkage of Blended Cement Mortars. Materials 2019;12:2603. https://doi:10.3390/ma12162603.
[28] Lade PV, Yammamuro JA, Bopp PA. Significance of particle crushing in granular materials. ASCE J Geotech Eng 1996;122(4):309–16.
[29] Lemougna PN, MacKenzie KJD, Melo UFC. Synthesis and thermal properties of inorganic polymers (geopolymers) for structural and refractory applications from volcanic ash. Ceram Int 2011;37(8):3011–8.
[30] Lemougna PN, Wang KT, Tang Q, Nzeukou AN, Billong N, Chinje Melo U, et al. Review on the use of volcanic ashes for engineering applications. Resour Conserv Recycl 2018;137:177–90.
[31] Liu X, Yang J, Wang G, Chen L. Small-strain shear modulus of volcanic granular soil: An experimental investigation. Soil Dyn Earthquake Eng 2016;86.
[32] Liu X, Zhang M, Shao L, Chen Z. Effect of volcanic ash filler on thermal viscoelastic property of SBS modified asphalt mastic. Constr Building Mat 2018;190:495–507.
[33] Mañosa J, Serrano-Conte J, Maldonado-Alameda A, Aulinas M, Chimenos JM. Pyroclastic volcanic ash as a potential precursor of alkali-activated binders – A case study from Tajogaite (La Palma, Canary Islands) volcano eruption. J Building Eng 2023;72:106623. https://doi.org/10.1016/j.jobe.2023.106623.
[34] Martin JD. 2004. XPowder: a software package for powder X-ray diffraction analysis. Qualitative, quantitative and microtexture. www.xpowder.com.
[35] Martinez I. 2022. Environmental impact of volcanic ash from La Palma (2021 event) an its revaluation in zeolitic materials. MSc thesis Faculty of Geology, UCM.
[36] Meyer V, Larkin T, Pender M. The shear strenght and dynamic shear stiffness of some New Zealand volcanic ash soils. Soils Found 2005;45(3):9–20. https://doi.org/10.3208/sandf.45.3_9.
[37] Miraki H, Shariatmadari N, Ghadir P, Jahandari S, Tao Z, Siddique R. Clayey soil stabilization using alkali-activated volcanic ash and slag. J Rock Mech Geotech Eng 2021. https://doi.org/10.1016/j.jrmge.2021.08.012.
[38] Miura S, Yagi K, Asonuma T. Deformation-strength evaluation of crushable volcanic soils by laboratory and in-situ testing. Soils Found 2003;43(4):47–57.
[39] Orense RP, Zapanta A, Hata A, Towhata I. Geotechnical characteristics of volcanic soils taken from recent eruptions. Geotech Geol Eng 2006;24:129–61. https://doi.org/10.1007/s10706-004-2499-y.
[40] Pallares C, Fabre D, Thouret JC, Bacconnet C, Charca-Chura JA, Martelli K, Talon A, Yanqui-Murillo C. 2015. Geological and geotechnical characteristics of recent lahar deposits from El Misti volcano in the city area of Arequipa, South Peru. Geotech Geol Eng. https://doi.org/10.1007/s10706-015-9848-x.
[41] Pankhurst MJ, Scarrow JH, Barbee OA, Hickey J, Coldwell BC, Rollinson GK, Rodríguez-Losada JA, Martín Lorenzo A, Rodríguez F, Hernández W, Calvo Fernández D, Hernández PA, Pérez N. M. 2022. Rapid response petrology for the opening eruptive phase of the 2021 Cumbre Vieja eruption, La Palma, Canary Island. Volcanica 5(1):1–10 https://doi.org/10.30909/ vol.05.01.0110.
[42] Presa L, Rosado S, Peña C, Martin DA, Costafreda JL, Astudillo B, et al. Volcanic Ash from the Island of La Palma, Spain: An experimental study to establish their properties as pozzolans. Processes 2023;11:657. https://doi.org/10.3390/pr11030657.
[43] Rendon MI, Viviescas JC, Osorio JP, Hernandez MS. Chemical, Mineralogical and Geotechnical Index Properties Characterization of Volcanic Ash Soils. Geotech Geol Eng 2020;38:3231–44. https://doi.org/10.1007/s10706-020-01219-3.
[44] Rifa A, Yasufuku N. Effect of volcanic ash as substitution material for soil stabilization in view point of geo-environment. In Ground Impr Geos GSP ASCE 2014;238:138–47.
[45] Robayo-Salazar RA, Mejía de Gutiérrez R. Natural volcanic pozzolans as an available raw material for alkali-activated materials in the foreseeable future: A review. Constr Building Mat 2018;189:109–18. https://doi.org/10.1016/j.conbuildmat.2018.08.174.
[46] Romero-Mancilla PE, Montenegro-Cooper JM, King RW, Lapeña-Mañero P, García-Casuso C. Experimental Investigation on the Influence of Oven-Drying on the Geotechnical Properties of Volcanic Ash-Derived Residual Soils. Appl Sci 2021;11:11708.
[47] Sanjuan MA, Frias M, Monasterio M, Garcia-Gimenez R, Vigil de la Villa R, Alamo M. 2023. Volcanic ash from La Palma (Canary Islands, Spain) as Portland cement constituent. J. Building Eng. https://doi.org/10.1016/j.jobe.2023.107641.
[48] Sayyah MA, Abrishami S, Dastpak P, Dias D. Behaviour of volcanic ash-soil mixtures under one-dimensional compression testing. Sci Rep 2022;12:14524. https://doi.org/10.1038/s41598-022-18767-8.
[49] Seguel O, Horn R. Mechanical behavior of a volcanic ash soil (Typic Hapludand) under static and dynamic loading. Soil Tillage Res 2005;82:109–16.
[50] Serra MF, Conconi MS, Suarez G, Aglietti EF, Rendtorff NM. Volcanic ash as flux in clay based triaxial ceramic materials, effect of the firing temperature in phases and mechanical properties. Ceram Int 2015;41:6169–77.
[51] Shariatmadari N, Hasanzadehshooiili H, Ghadir P, Saeidi F, Moharami F. 2021. Compressive Strength of Sandy Soils Stabilized with Alkali-Activated Volcanic Ash and Slag. J Materials Civil Eng, ASCE, ISSN 0899-1561, Vol. 33 (11).
[52] Siddique R. Properties of concrete made with volcanic ash. Resour Conserv Recycl 2012;66:40–4. https://doi.org/10.1016/j.resconrec.2012.06.010.
[53] Supriyo H, Matsue N, Yoshinaga N. Chemical and Mineralogical Properties of Volcanic Ash Soils from Java Soil. Sci Plant Nutr 1992;38(3):443–57.
[54] Stewart C, Damby DE, Tomasek I, Horwell CJ, Plumlee GS, Armienta MA, et al. Assessment of leachable elements in volcanic ashfall: a review and evaluation of a standardized protocol for ash hazard characterization. J Volcanology Geothermal Research 2020;392:106756. https://doi.org/10.1016/j.jvolgeores.2019.106756.
[55] Tchakoute HK, Elimbi A, Yanne E, Djangang CN. Utilization of volcanic ashes for the production of geopolymers cured at ambient temperature. Cement Concr Compos 2013;38:75–81.
[56] Thiha S, Lertsuriyakul C, Phueakuphum D. Shear Strength Enhancement of Compacted Soils Using High-Calcium Fly Ash-Based Geopolymer. Geotec. Const. Mat. & Env Int J GEOMATE 2018;Vol. 15, Iss 48:1–9. https://doi.org/10.21660/2018.48.35692.
[57] UNE 103-105:1993. Geotechnic. Determination of minimum density of a sand.
[58] UNE 103-106:1993. Geotechnic. Determination of maximum density of a sand by the ramming method.
[59] UNE 103-406:2006. Geotechnic. Collapse test in soils.
[60] UNE 103-500:1994. Geotechnic. Compactation test. Standard Proctor.
[61] Vandenberghe RE, de Resende VG, da Costa GM, De Grave E. Study of loss-on-ignition anomalies found in ashes from combustion of iron-rich coal. Fuel 2011;89.
[62] Volcanes https://www.eitb.eus/es/tag/volcanes/.
[63] Vu DH, Wang KS, Xuan Nam B, Hoang Bac B, Chu TC. Preparation of humidity-controlling porous ceramics from volcanic ash and waste glass. Ceram Int 2011;37:2845–53.
[64] Yankwa Djobo JN, Elibli A, Tchakoute HK, Kumar S. Mechanical properties and durability of volcanic ash based geopolymer mortars. Constr Building Mat 2016;124:606–14. https://doi.org/10.1016/j.conbuildmat.2016.07.141.
[65] Zhou S, Lu C, Zhu X, Li F. Upcycling of natural volcanic resources for geopolymer: Comparative study on synthesis, reaction mechanism and rheological behavior. Constr Building Mat 2021;268:121184. https://doi.org/10.1016/j.conbuildmat.2020.121184.